Naval Medical Research Institute
8901 Wisconsin Avenue
Bethesda, MD 20889-5607

NMRI 95-59 October 1995

FINAL ASSESSMENT OF THE FEASIBILITY OF A SYSTEM FOR ACOUSTICALLY DETECTING STATIONARY GAS BUBBLES USING TIME DELAY SPECTROMETRY

G. W. Albin
W. H. Mints
J. S. Colton

Naval Medical Research
and Development Command
Bethesda, Maryland 20889-5606

Department of the Navy
Naval Medical Command
Washington, DC 20372-5210

NOTICES

The opinions and assertions contained herein are the private ones of the writer and are not to be construed as official or reflecting the views of the naval service at large.

When U. S. Government drawings, specifications, or other data are used for any purpose other than a definitely related Government procurement operation, the Government thereby incurs no responsibility nor any obligation whatsoever, and the fact that the Government may have formulated, furnished or in any way supplied the said drawings, specifications, or other data is not to be regarded by implication or otherwise, as in any manner licensing the holder or any other person or corporation, or conveying any rights or permission to manufacture, use, or sell any patented invention that may in any way be related thereto.

Please do not request copies of this report from the Naval Medical Research Institute. Additional copies may be purchased from:

National Technical Information Service
5285 Port Royal Road
Springfield, Virginia 22161

Federal Government agencies and their contractors registered with the Defense Technical Information Center should direct requests for copies of this report to:

Defense Technical Information Center
Cameron Station
Alexandria, Virginia 22304-6145

TECHNICAL REVIEW AND APPROVAL

NMRI 95-59

The experiments reported herein were conducted according to the principles set forth in the current edition of the "Guide for the Care and Use of Laboratory Animals," Institute of Laboratory Animal Resources, National Research Council.

This technical report has been reviewed by the NMRI scientific and public affairs staff and is approved for publication. It is releasable to the National Technical Information Service where it will be available to the general public, including foreign nations.

THOMAS J. CONTRERAS
CAPT, MSC, USN
Commanding Officer
Naval Medical Research Institute

REPORT DOCUMENTATION PAGE

Form Approved
OMB No. 0704-0188

1. AGENCY USE ONLY (Leave blank)	2. REPORT DATE	3. REPORT TYPE AND DATES COVERED
	1995	Technical report

4. TITLE AND SUBTITLE

Final assessment of the feasibility of a system for acoustically detecting stationary gas bubbles using time delay spectrometry

5. FUNDING NUMBERS

PE - 63713N
PR - M0099
TA - 01A
WU - 1510

6. AUTHOR(S)

Albin GW; Mints WH; Colton JS

7. PERFORMING ORGANIZATION NAME(S) AND ADDRESS(ES)

Naval Medical Research Institute
Commanding Officer
8901 Wisconsin Avenue
Bethesda, Maryland 20889-5607

8. PERFORMING ORGANIZATION REPORT NUMBER

NMRI 95-59

9. SPONSORING/MONITORING AGENCY NAME(S) AND ADDRESS(ES)

Naval Medical Research and Development Command
National Naval Medical Center
Building 1, Tower 12
8901 Wisconsin Avenue
Bethesda, Maryland 20889-5606

10. SPONSORING/MONITORING AGENCY REPORT NUMBER

DN241126

11. SUPPLEMENTARY NOTES

12a. DISTRIBUTION/AVAILABILITY STATEMENT

Approved for public release; distribution is unlimited.

12b. DISTRIBUTION CODE

13. ABSTRACT (Maximum 200 words)

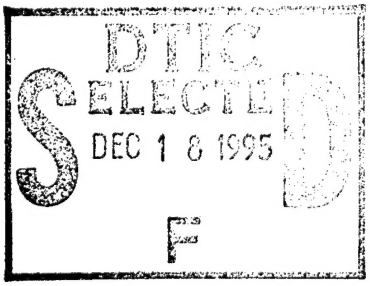

14. SUBJECT TERMS

bubbles; decompression sickness; ultrasound; time delay; spectrometry; medical imaging; audiography

15. NUMBER OF PAGES

16. PRICE CODE

17. SECURITY CLASSIFICATION OF REPORT	18. SECURITY CLASSIFICATION OF THIS PAGE	19. SECURITY CLASSIFICATION OF ABSTRACT	20. LIMITATION OF ABSTRACT
Unclassified	Unclassified	Unclassified	Unlimited

REPORT DOCUMENTATION PAGE

Form Approved
OMB No. 0704-0188

1. AGENCY USE ONLY (Leave blank)	2. REPORT DATE	3. REPORT TYPE AND DATES COVERED
	October 1995	Technical 10-1-93 to 10-1-94

4. TITLE AND SUBTITLE
Final assessment of the feasibility of a system for acoustically detecting stationary gas bubbles using time delay spectrometry.

5. FUNDING NUMBERS
PE - 63713N
PR - M0099
TA - .01A
WU - 1510

6. AUTHOR(S)
Albin, G.W., W.H. Mints, J.S. Colton

7. PERFORMING ORGANIZATION NAME(S) AND ADDRESS(ES)
Naval Medical Research Institute
Commanding Officer
8901 Wisconsin Avenue
Bethesda, Maryland 20889-5607

8. PERFORMING ORGANIZATION REPORT NUMBER
NMRI 95-

9. SPONSORING / MONITORING AGENCY NAME(S) AND ADDRESS(ES)
Naval Medical Research and Development Command
National Naval Medical Center
Building 1, Tower 12
8901 Wisconsin Avenue
Bethesda, Maryland 20889-5606

10. SPONSORING / MONITORING AGENCY REPORT NUMBER
DN241126

11. SUPPLEMENTARY NOTES

12a. DISTRIBUTION / AVAILABILITY STATEMENT
Approved for public release; distribution is unlimited.

12b. DISTRIBUTION CODE

13. ABSTRACT *(Maximum 200 words)*

The Jet Propulsion Laboratory swept-frequency bubble detector has been discussed in previous reports (Albin et al., 1991 and 1992). Physically similar to the familiar ultrasound scanning devices for medical imaging, it was designed to nondestructively detect stationary resonant bubbles of < 7 μm diameter using time delay spectrometry (TDS), but proved insufficiently sensitive to do so. This report is a discussion of whether that system could be redesigned successfully. Techniques to improve the signal/noise (S/N) ratio are explored, including exciting larger bubbles at lower frequency. Analysis indicates that the new system should indeed be sensitive enough to detect resonant bubbles in the 40-400 μm diameter range. However, the shift to lower frequencies brings with it a problem peculiar to TDS systems: there are multi-path signal arrivals, which in TDS systems translates into a loss of resolution in the time domain. Because identifying the resonance frequencies depends upon the temporal coherence of the signal, the technique cannot work at low frequencies. Various strategies for maintaining time resolution at lower frequencies are discussed, along with the reasons why they will not work. Adequate time resolution is realized at much higher frequencies, but the S/N ratio at those frequencies would be satisfactory only if the acoustical scanning signal were of such high amplitude that the measurement would be destructive to the bubbles and their milieu. It does not appear possible at present to design a TDS system that is simultaneously sensitive enough for the proposed application **and** nondestructive--such a device will become possible in the future if acoustic transducer sensitivities are improved by several orders of magnitude.

14. SUBJECT TERMS
bubbles, decompression sickness, ultrasound, time delay spectrometry, medical imaging, audiography

15. NUMBER OF PAGES
52

16. PRICE CODE

17. SECURITY CLASSIFICATION OF REPORT	18. SECURITY CLASSIFICATION OF THIS PAGE	19. SECURITY CLASSIFICATION OF ABSTRACT	20. LIMITATION OF ABSTRACT
Unclassified	Unclassified	Unclassified	Unlimited

TABLE OF CONTENTS

LIST OF FIGURES

ACKNOWLEDGEMENTS

We are indebted to George Goehring, Walt Long, and William Tetrault for expertly fabricating equipment. We have appreciated the insights that Paul Massell has had into fast Fourier transformation. We are grateful to Jeff Frank of Wesmar Defense Products, and to Dick Hugus and Larry Ivey of the Naval Research Laboratory, for many helpful discussions of sonar transducers. Richard Price of the Aberdeen Proving Grounds had some especially valuable insights into noise-induced hearing loss. Thanks to Susan Mannix for editorial work on this document.

This work was supported by Naval Medical Research and Development Command Work Unit No. 63713N M0099.01A-1510. The opinions and assertions contained herein are the private ones of the author and are not to be construed as official or reflecting the views of the United States Navy or the naval service at large.

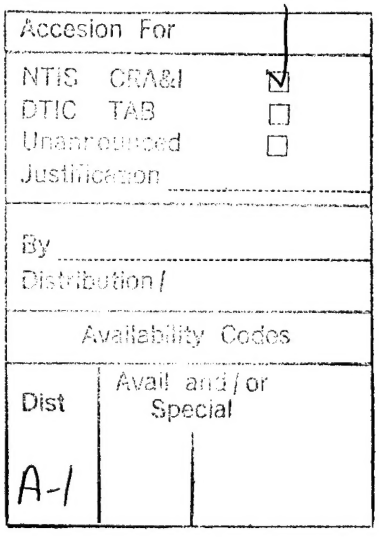

BACKGROUND

Development work on the Jet Propulsion Laboratory (JPL) swept-frequency bubble detector has been described in two previous NMRI Technical Reports (Albin et al. 1991, Albin et al., 1992). Briefly, the work has been directed at building a working instrument for acoustical scanning using time delay spectrometry (TDS), a signal processing technique that yields information on the frequency response of the acoustical target(s) and their distances from the probes. The frequency response information is intended to enable identification of the resonance frequencies, and thus the sizes, of bubbles. It is possible to use the instrument so that the output signal consists of one component of the harmonic distortion present in the backscattered acoustical energy: the concept is that harmonic distortion, being generated only by nonlinear oscillations, indicates the presence of a resonant gas phase. Thus, the bubble detector has potential for studying the stationary gas phases in tissue that may cause decompression sickness. The operating frequency band is about 1-7 megahertz (MHz) and is limited by the acoustical transducers. This range corresponds to the main resonance frequencies of bubbles in water less than ~7 μm in diameter.

It was noted in a previous report (Albin et al., 1992) that the harmonic distortion generated internally by nonlinearities within the measurement system was roughly the same as the contribution from a nonlinearly oscillating gas bubble. (The expected bubble behavior is based on a fairly detailed mathematical model of a spherical bubble oscillating at its resonance frequencies.) In other words, the signal/noise (S/N) ratio is approximately equal to one, if "noise" is taken to be the distortion intrinsic to the measurement system. This result is based on an analysis that is deliberately skewed to show the existing instrument in a favorable

light; in practice, S/N would probably be substantially worse when scanning biological samples. Another problem is that bubbles of less than 7 μm diameter are quite transient, tending to either implode or to grow out of measurement range within less than 1 second, in the absence of some stabilization mechanism (two proposed mechanisms are stabilization in a crevice or by a radius-dependent surface tension, but it has not been determined that either phenomenon occurs *in vivo*). The obvious implication is that the prospects of obtaining a recognizable signal are slim.

To improve the S/N ratio, three strategies seemed promising. First, it is possible to simplify the design by eliminating several components, one of which is highly nonlinear. No capabilities will be lost in this proposed hardware change. Second, the hardware can be redesigned for operation at lower frequencies, which would excite larger bubbles to resonance; larger bubbles have larger scattering cross sections, and therefore would deliver more energy to the receiving acoustical transducer (to a rough approximation, the resonance frequencies of a spherical bubble are inversely proportional to the bubble's radius, and the amplitude of distortion products in the sound radiated back from it increases sharply with bubble radius). This second strategy has the incidental benefit that the stability of bubbles inherently increases with size, making it easier to generate useful calibration standards. Third, it *may* be possible to implement more sophisticated signal processing techniques to separate weak signals from white noise and measurement distortion. This last strategy is somewhat speculative and its implementation would require specialized signal processing expertise.

In this report we consider the execution of the first two of the above measures, estimate the performance capabilities of the bubble detector upon their completion, and draw a conclusion as to the feasibility of building a TDS system for studying bubbles *ex vivo*. Operation at lower frequencies is found to be necessary if adequate sensitivity is to be realized at reasonably safe input sound pressure levels. However, at lower frequencies there is a loss of spatial resolution because of multipath signal arrivals, for reasons peculiar to the TDS method. In any TDS system, spatial resolution is equivalent to temporal resolution of the received signal and meaningful amplitude demodulation is impossible without adequate temporal resolution. Therefore, at low frequencies the system is not useful for determining either the range of bubbles (their distances from the probes) or their sizes (which can be deduced from their resonance frequencies that are found via the amplitude demodulation)*. In other words, the information that this instrument was intended to deliver is not available at low frequencies; and at high frequencies it is nominally available. In practice, it is buried in the system's internally generated noise and distortion. Various strategies for maintaining time resolution at lower frequencies have been considered and will be discussed; they will not work. It does not appear possible at present to design a TDS system that is simultaneously sensitive enough for the proposed application *and* nondestructive. Such a device might be possible in the future if acoustic transducer sensitivities are improved by several orders of magnitude, as this would mean a stronger signal at the receiving transducer without the need for boosting the input voltage.

* The authors recognize that these issues, being specific to TDS systems, are probably obscure to most readers; the authors will attempt in a later section to explain the ideas in sufficient detail.

A non-TDS system that should enable detection of bubbles is discussed briefly. It would not provide any range information on bubbles but, theoretically, should identify their resonance frequencies.

SELECTING THE OPERATING FREQUENCY BAND

Expected resonance frequencies

The aim of this research is to find and learn about extravascular bubbles whose locations and sizes make them important to the etiology of decompression sickness. The relevant size range then determines the frequency range of interest.

Information is scarce on what size bubbles exist *in vivo* after decompression. After all, that is one question that the bubble detector is intended to answer. Francis et al. (1988, 1990) counted and sized the bubbles in the spinal cords of dogs that had been decompressed from 300 feet of seawater (fsw). Each dog was killed by perfusion fixation only after an 80% reduction from baseline in the somatosensory evoked potential (SEP). Therefore, the physiological effects obviously were more severe than for a routine human dive. The bubbles tended to be large. In the white matter, elongated bubbles were observed whose average volume equalled the volume of a spherical bubble of about 160 μm diameter. The bubbles occupied about 0.3% of the volume in the white matter. The number of bubbles present is staggering: it would take about 1300 such bubbles per cm^3 to bring the void fraction up to 0.3%.

Gersh (1945) found bubbles with major axes as long as 3 mm in various freeze-dried tissues taken from guinea pigs after they had undergone severe decompression schedules.

Wagner (1945) found bubbles in some of the cats that he had subjected to severe decompression, but did not report their sizes.

Hills and Butler (1981) found intravascular bubbles in dogs ranging from 20 to 180 μm diameter. The size measurements were done *ex vivo* on withdrawn blood. There may actually have been smaller bubbles present *in vivo* , but it is highly likely that they would have either disappeared or grown larger than 20 μm before it was possible to size them. Therefore, the results in this paper should not be taken to indicate the low end of the size range of intravascular bubbles.

None of the information summarized above is convincing evidence of the sizes of extravascular bubbles that might exist during or after typical U.S. Navy dives.

The resonance frequency of a population of bubbles is different from the resonance frequency of just one of the bubbles alone. The theory of bubble cloud dynamics has been advanced in several recent papers (Omta, 1987; d'Agostino and Brennan, 1988; Smereka and Banerjee, 1988; d'Agostino and Brennan, 1989; Prosperetti et al., 1989; Lu et al., 1990; Kumar and Brennan, 199; Yoon et al., 1991; Prosperetti et al., 1993; and Sarkar and Prosperetti,1993). For a cloud of *same-sized* bubbles, the resonance frequency is less than for any one of the bubbles in isolation. This effect becomes appreciable when the bubbles occupy 0.001% or more of the total volume.

Practical considerations

If there is a lack of convincing evidence that would enable one to decide *a priori* about what sizes are important, then one might choose a frequency band through a practical

consideration of what band might be easiest to work in. In other words, in what band would there be the best chance of finding gas phases during decompression?

It already has been noted that larger bubbles scatter more energy, and that larger bubbles resonate at lower frequencies. Whereas the previous version of the bubble detector did not work because it was not sensitive enough, it is reasonable to consider moving to a lower frequency band in order to enhance the sensitivity.

Signal level is also reduced by attenuation of the sound waves in the medium surrounding the bubbles ("transmission loss"). This loss is less important at lower frequencies; the published data on attenuation of sound suggest that it has something like a direct proportionality with frequency in soft tissues, although the data are quite scattered. For signals less than ~300 kHz and two-way transmission path lengths of less than 10 cm, attenuation is no more than a few tenths of a decibel (dB) in soft tissue, which is negligible (Daft et al., 1989; Goss et al., 1980). Therefore, concern about sensitivity again leads one to favor lower frequencies.

Safety factors: Noise-induced hearing loss, cavitation, rectified diffusion

There are reasons to favor operation at lower frequencies. However, if the operating band is low enough to approach or even overlap the audible band, then possible hearing damage to the subject (and maybe to the operator, as well) must be considered.

If the operating band is higher than the audible band, there still is a concern about the generation of subharmonics by the transducers or by the ears themselves. Subharmonic components in the response of guinea pig ears to high amplitude sounds has been observed at levels of at least 50 dB below the fundamental (Dallos, 1973).

Sound will be transferred from the transmitting transducer to the ear mainly by bone conduction. It will be attenuated drastically by reflection at the bone/air interface in the inner ear. There will be a minimum of 37 dB loss in acoustic intensity in the transmission across this interface; this is the loss calculated for a beam normally incident to a planar interface using the mechanical impedance data from Buddemeyer (1975). If the incident sound is evenly distributed over all angles, then the global transmission loss equals its average value over all angles of incidence:

$$T_{avg} = (2/\pi) \int_0^{\pi/2} T(\theta)\, d\theta \qquad [1]$$

$T(\theta)$ is the intensity transmission coefficient, equal to $I_T\ (\theta)/I_i$, where the subscripted T and i denote transmitted and incident sound, respectively. An expression for $T(\theta)$ from Kinsler et al., (1982) is substituted into Equation 1 and the global transmission loss at the bone/air interface is estimated to be 39 dB. It is found by similar means that there will be an additional intensity loss of about 9.2 dB at the soft tissue/bone interface.

There is still further transmission loss between the projector and the ear resulting from geometrical attenuation and leakage through the skin into air. The actual transmission paths and losses would be extremely difficult to predict accurately, but will be very substantial given that the skin has a much greater surface area than the inner ear. Attenuation in tissue should be negligibly small at frequencies much less than 1 MHz.

It is generally accepted that noise-induced hearing loss within a given frequency band depends in a rather simple way on the energy present within that band, at least up to sound pressure levels of ~130 dB (Price, 1992). Therefore, a useful means of estimating auditory

hazard for our purposes is simply to calculate how much energy is generated at audible frequencies. The sonic energy depends on both the duration and the intensity of the sound. The duration of exposure to a subject whose tissue is being scanned by the bubble detector will be quite low relative to typical workplace exposures. To illustrate, consider that each frequency sweep probably will last on the order of 0.2 s, at a constant sweep rate in Hz/s. If the operating band is 100 kilohertz (kHz) and overlaps the audible range, then the exposure in the *widest* 1/3 octave within the nominal audible range, the 15.9 to 20 kHz band, lasts barely 8 msec. This is fairly short compared with the duration of, say, a howitzer report (Price and Kalb, 1991).

Another potential hazard is cavitation, which might occur during rarefaction (the negative half of the input pressure wave). Cavitation thresholds have been measured in water (Atchley et al., 1988; Crum et al., 1992). Their theoretical values have been calculated for nuclei stabilized in crevices (Atchley and Prosperetti, 1989) and stabilized by a surfactant (Atchley, 1989). Finally, a risk is posed by the possibility that existing bubbles will be made to grow by rectified diffusion (Atchley, 1988).

The risk of cavitation, rectified diffusion, and hearing loss depend on the pulse length, pulse repetition frequency (PRF), and sonic intensity. They will have to be evaluated once a specific projector and signal generator have been chosen for evaluation.

BASIC PRINCIPLES OF OPERATION OF THE TDS BUBBLE DETECTOR

A brief description of the TDS bubble detector is offered here. The reader should look to Albin et al. (1991) for a more comprehensive discussion.

Description of the signal path and signal processing

The bubble detector uses a transmit acoustic transducer, or projector, to scan its target area. The scanning signal is swept through some frequency band at a constant rate in $Hz \cdot time^{-1}$. A receive acoustic transducer, or hydrophone, detects the backscattered sound from any acoustic reflectors, including bubbles.

Because the input signal is swept-frequency, a constant frequency offset (f_{offset}) between the input signal and the *fundamental* component of the backscattered signal arises because of the transmission path delay (provided the reflector is stationary):

$$f_{out}^{fund}(t) = f_{in}(t) + f_{offset}$$

This f_{offset} is proportional to the two-way transmission path length. Likewise, the *2nd harmonic* distortion component of the backscattered signal is offset in frequency by the same amount f_{offset} from the quantity $2 \cdot f_{in}(t)$:

$$f_{out}^{2nd}(t) = 2 \cdot f_{in}(t) + f_{offset}$$

In the JPL bubble detector, a voltage of frequency $f_{in}(t)$ is sent to the projector; synchronously, a voltage of frequency, $2 \cdot f_{in}(t)$, is heterodyned with the signal from the hydrophone. The heterodyning can be thought of as a separation of the modulating frequency f_{offset} from the desired carrier frequency, $2 \cdot f_{in}(t)$. Appropriate bandpass filtering then removes the fundamental and all harmonic components that had been present in the signal from the hydrophone, except for the 2nd harmonic (i.e. the other carrier frequencies are filtered out). The filtering also removes all modulating frequencies outside the passband, meaning that it eliminates signals that are traceable to targets lying outside some selectable range of transmission path lengths.

The signal is next Fourier transformed and its frequency content indicates the transmission path lengths of the targets. This is somewhat analogous to measuring the range of a target using active sonar.

The signal is also amplitude demodulated. This shows how the amplitude varies with time during the scan, which reveals the dependency of the amplitude on the input frequency. In other words, the frequency response of the system comprising both the bubble and the bubble detector is computed. Sharp peaks in the frequency response should represent resonance frequencies. The size of a bubble can be estimated from its resonance frequencies.

The need for time-coherent output signals

Meaningful information on a bubble's range is available from the Fourier transformation *only* if the bandpass filtering removes signals that arrive at the hydrophone via indirect paths. By indirect, we mean those signals that have been reflected at surfaces other than the bubble's surface. Otherwise, the spectrum would show multiple offset frequencies for the same bubble, owing to multiple arrival times at the hydrophone.

By the same token, meaningful information on a bubble's size can be gotten from the amplitude demodulation only if the following condition is met: During data capture, the bubble must be excited to resonance *only* when the input signal is being swept through one of the bubble's resonance frequencies. This condition would not be met if other reflecting surfaces were too close to the bubble. During data capture, the bubble would be stimulated by reflected sound after being initially stimulated by sound arriving directly from the projector. It might resonate multiple times during data capture, so that multiple peaks would

be seen in the demodulated signal. Obviously, it would be difficult to sort out the true resonance frequencies from the spurious ones.

In a TDS system, the requirement of time-coherent output signals is equivalent to the requirement of adequate spatial resolution. Good spatial resolution is realized if signals arriving via indirect transmission paths are eliminated. Another way to put this is that multipath signal arrivals must be eliminated. This means that the bandpass filter must remove all signals with f_{offset} values greater than some value determined by the size and geometry of the medium that is to be interrogated. The factors that determine spatial resolution and the way in which poor spatial resolution affects a measurement are unique to TDS. A later section will address how the available resolution is calculated.

ALTERING THE SYSTEM CONFIGURATION TO MINIMIZE HARMONIC DISTORTION

The bubble detector can be operated such that the output signal is a component of the harmonic distortion in the energy backscattered from acoustical targets. More specifically, it is expected that the 2nd harmonic component will be studied predominantly, because this is the largest of the harmonics in the sound scattered by a vibrating bubble.

The instrument's capacity for measuring harmonic distortion depends on generating two synchronous swept frequency signals in a way that the ratio of their frequencies is some constant integer. If the 2nd harmonic component is of interest, then the necessary ratio is two. The existing instrument generates these synchronous signals by splitting a swept frequency signal and sending one part to an analogue frequency changer. This is shown in the block diagram of Figure 1. Here, the frequency of the signal of interest at various stages

of the signal path is labelled in terms of the "source frequency" (f_s) ; the system is shown as operating in 2nd harmonic mode. The output signal from this frequency changer has a frequency half that of the input signal; as shown in Figure 1, the output feeds into a power amplifier whose output goes to the transmitting transducer. The problem with the pictured system is that the 2nd harmonic distortion generated by the existing frequency changer is at least 0.5% of the fundamental, i.e. 46 dB below the fundamental, by direct measurement. This is a major contribution to the total harmonic distortion of the bubble detector. The significance is that the system's sensitivity as a detector of 2nd harmonic distortion in the sound radiated by bubbles is limited by the level of its internally generated 2nd harmonic distortion.

Alternatively, the two synchronous swept-frequency signals could be generated by a suitably flexible two-channel signal synthesizer. For measuring a harmonic distortion product, the frequency band of one channel's output could be set at an integral multiple of the other channel's: two for measuring the 2nd harmonic, three for the 3rd harmonic, etc. A good, modern synthesizer would generate signals of considerably higher purity than those produced by the existing equipment.

The new configuration of the system is diagrammed in Figure 2. Again, the signal frequency is labelled at various stages. Channel A of the synthesizer feeds into the projecting transducer. Channel B feeds into a mixer. The signal received at the hydrophone is amplified and then fed into the same mixer. The mixer output is an intermediate frequency (IF) signal that goes to a Hewlett Packard 3561A spectrum analyzer. Selection of a suitable signal synthesizer will be discussed in the following section.

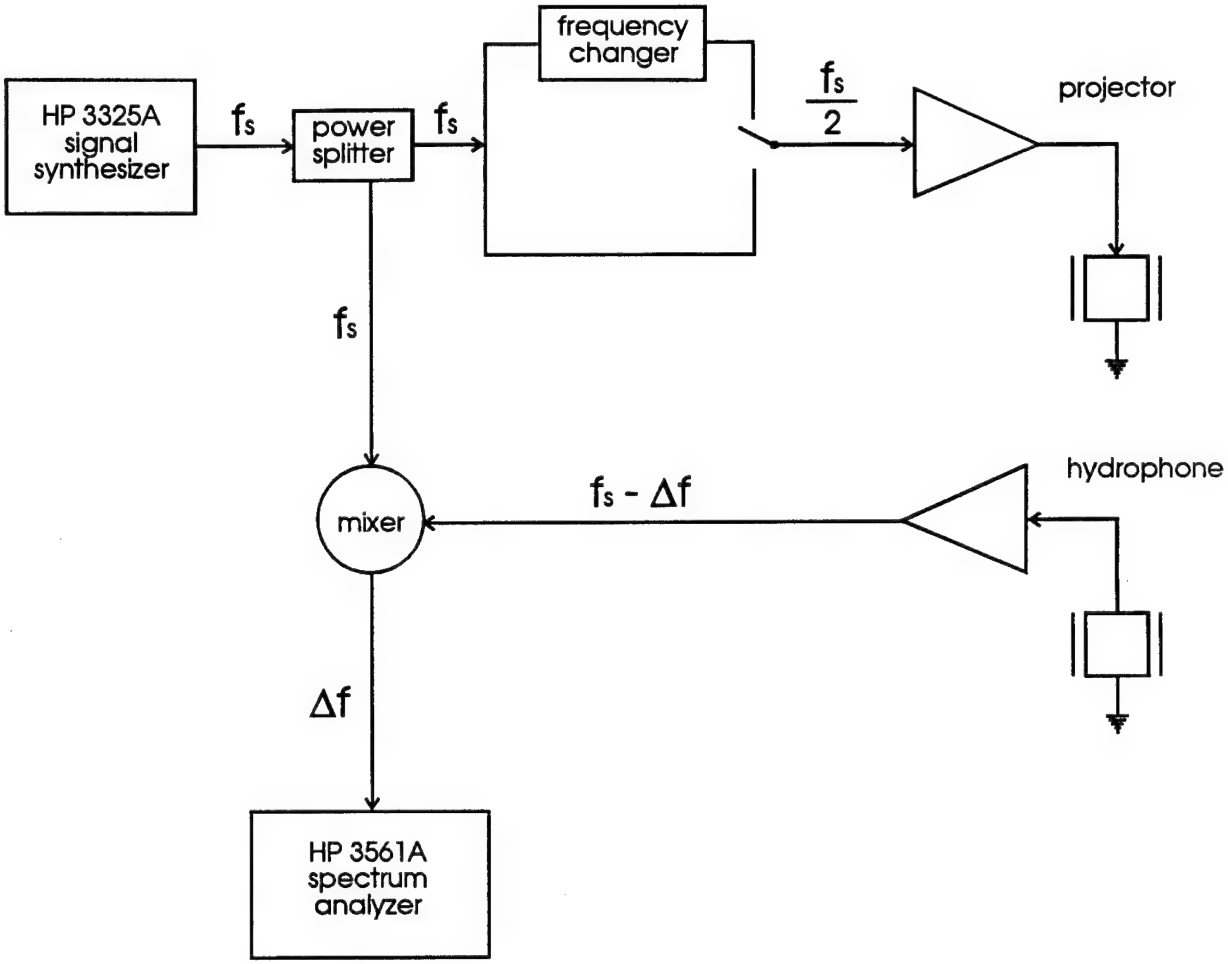

Figure 1: Existing system

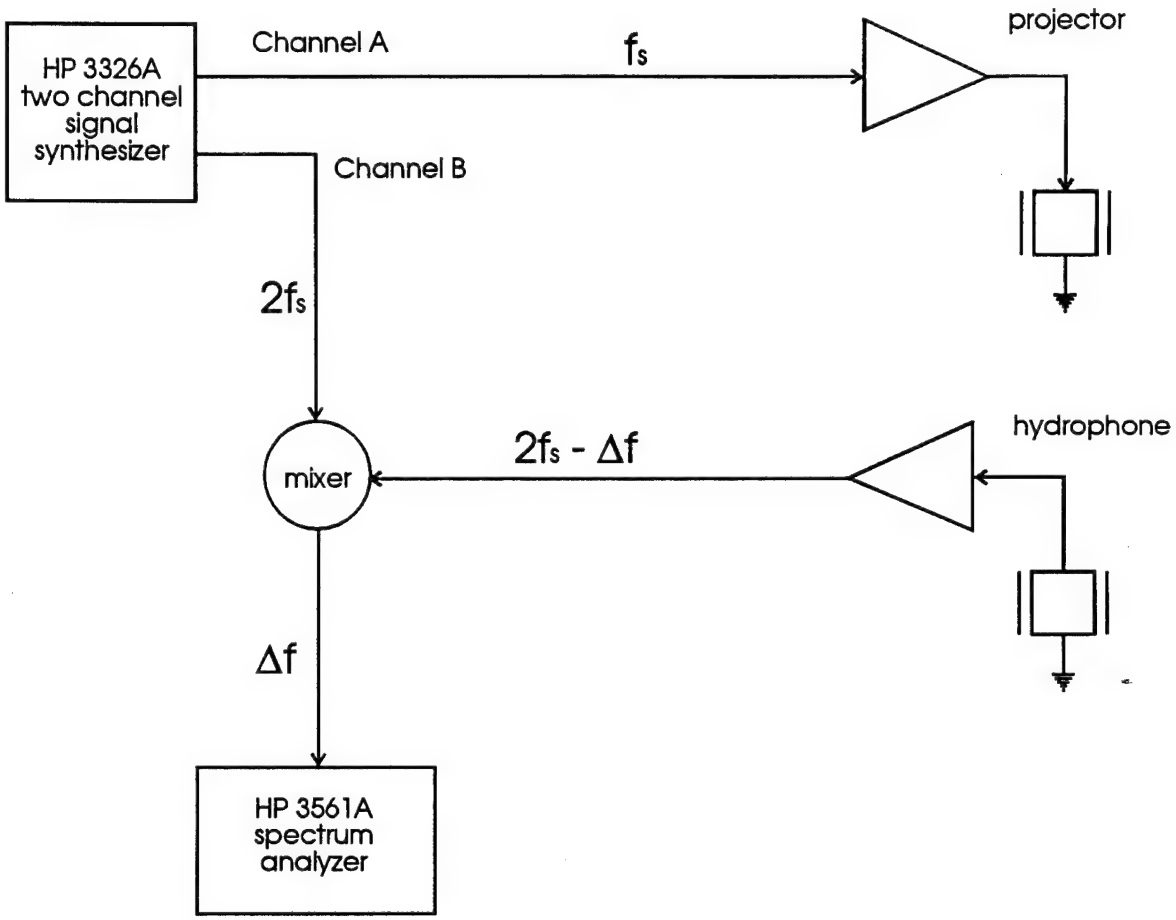

Figure 2: Proposed system

SELECTING THE HARDWARE

In this section, components are discussed that represent the current state of the art in signal processing. They would be parts in a redesigned TDS-based bubble detector. In subsequent sections, the system's expected operating characteristics will be considered.

All connections are made with standard R/G58 coaxial 50-Ω BNC cables.

Acoustic transducers

The desired transducers are as broadband and sensitive as possible. The frequency response of the projector should extend as low as 20 kHz when it is coupled with a medium acoustically similar to water or biological tissue. It is desirable for the hydrophone to respond to a frequency band twice as high as the band of the projected signals. The available transducers that meet these criteria are piezoelectric ceramic units that are designed for sonar applications.

The Naval Research Laboratory (NRL) in Orlando FL offers calibrated sonar transducers for lease. Two models seem particularly well-suited for use in the bubble detector. Model F41 is an array of 12 lead zirconate-titanate (PZT) crystals. When used as a projector, it has a nominal operating band of 15-150 kHz, which encompasses the main resonance frequencies of free bubbles in water that have diameters of ~40-400 μm. It accepts input levels of up to 200 Vrms (V root mean squared). Model E27 is an array of 7 PZT crystals, and has a nominal band of 80-700 kHz as a hydrophone. Each transducer presents an equivalent series impedance near 50 Ω . They are in separate housings and so can be positioned relative to one another in whatever orientation minimizes stray signals from non-bubble scatterers. Specifications are not provided for harmonic distortion and non-

harmonically related noise. Because of their operating frequency bands, it makes sense to use the F41 as the projector and the E27 as the hydrophone.

When the desirable performance characteristics have been better defined, it may be appropriate to seek customized transducers from NRL or one of the commercial sonar equipment manufacturers.

Two-channel signal synthesizer

The Hewlett-Packard 3326A appears to have the necessary capabilities. Its claimed harmonic distortion limit, more than 70 dB below the fundamental for any harmonic at any output level and frequency, is a vast improvement over the performance of the present hardware. Spot measurements of a sample unit indicate that the 2nd harmonic distortion component is actually ~90 dB below the fundamental at 40 kHz. All non-harmonically related output signals are less than -80 dB relative (*re*) to the fundamental, or less than 38 decibels relative to 1 mV (dBm) at the maximum output level. The non-harmonic noise important in our application is white noise, and its level is specified to be -90 dBm.

The output level is variable from 1 μV peak-peak to 10 V peak-peak (0.35 μVrms to 3.5 Vrms). It will be shown that this is high enough to obviate an additional amplifier. Therefore the HP 3326A replaces not only the signal splitter and frequency changer, but also the power amp.

Low-noise amplifier (LNA)

The model SR560 low-noise amplifier from Stanford Research Systems in Sunnyvale, CA generates a 2nd harmonic component no higher than -78 dB *re* the fundamental for a 40 kHz input, determined by spot measurements on a sample unit. It contributes is 4 nVrms per

root Hz (that is, 4 nV multiplied by the square root of the operating bandwidth) to the white noise when the source impedance is "low", as ours is. The amplifier saturates at an input level of 1.5 V peak, or +15.5 dBm. This amplifier has a variable gain of 1 to 50,000 (0 to 94 dB). It has a series of single-pole filters that can be configured to provide high-pass, low-pass, or bandpass filtering, with 6 or 12 dB/octave rolloff and selectable cutoff frequencies.

Signal mixer

The output from the hydrophone will be amplified and sent to the mixer, where it will be mixed with the output of channel B of the signal synthesizer (see Figure 2). Several low-distortion mixers are available from Mini-Circuits (Brooklyn, NY). The most appropriate model can be selected by considering the expected input signal levels. The chosen models overload when the signal level at the "local oscillator" port (or LO port, which is fed from channel B of the signal synthesizer) is +7 to +23 dBm or when the level at the "radio frequency" port (RF port, fed from the low noise amplifier) is +1 to +15 dBm, depending on the model. Therefore, the mixer limits the signal level for the overall system; it overloads at a lower level than anything else does. The chosen models have 2nd harmonic intermodulation distortion figures of no worse than -76 dB relative to the output level for the expected input levels, and they increase the white noise by about 6 dB .

OVERALL SYSTEM PERFORMANCE: PREDICTED DYNAMIC RANGE

A single-bubble target

Dynamic range is defined as the range of signal levels that a system can process without being affected at low levels by internally generated noise or at high levels by

internally generated distortion. It is a measure of the maximum possible S/N ratio, and measuring bubbles will be possible only if the dynamic range of the instrument is wide enough. The dynamic range necessary for a successful measurement depends on what signal levels are encountered at the hydrophone. Dynamic range is determined by the level of the *weakest* signal to be resolved without disappearing into the noise floor, and the level of the *strongest* signal to be resolved without overloading the electronics. (In our case, overload at the mixer input would generate harmonic distortion products likely to obscure the signal of interest). It is easy to identify what sorts of signals define the requisite dynamic range: The weakest signal of importance will be the 2nd harmonic component of the sound radiated from a single resonant bubble, and the highest voltage likely to be encountered at the hydrophone would result from strong scattering by a hard target in the transmission path.

The estimation of these voltage levels is straightforward if one knows the gains of the transducers and has a reliable model for acoustic scattering by a resonant bubble. The procedure will be summarized here and is shown in detail in the Appendix, which is a document generated using Mathcad version 3.1 software.

Typical performance characteristics for their acoustic transducers are available from NRL in advance of sale. For the model F41 projector they provide the transmitting voltage response (TVR) in μPa/Volt (V), measured in the free field, on-axis, 1 m from the transducer face. For the F41 transducer, 1 m is in the "far field", that is, the beam is spherically divergent. The reported TVR must be adjusted upward in our case because the targets of interest are much closer than 1 m: We assume a target distance of 3 cm. We use an equation from Bobber (1970) to estimate the frequency band over which a 3 cm-distant target is in the

near field. Another equation from Bobber is used to extrapolate the near-field TVR from the far-field TVR at these frequencies. Over most of the operating band, 3 cm is in the far field, and so at these frequencies the TVR at 3 cm is extrapolated from the TVR at 1 m using the inverse relationship between distance and pressure amplitude. Also provided by NRL is a typical free-field voltage sensitivity (FFVS), measured in V/μPa, for the model E27 hydrophone.

The TVR of the projecting transducer peaks at 150 kHz, the main resonance frequency of the crystals. It rolls off sharply (about 16 dB per octave) with decreasing frequency. The FFVS of the hydrophone is almost flat above the main resonance frequency of its crystals, 80 kHz.

Let us define a "scattering efficiency" between the projector and the hydrophone as

$$\frac{\textit{amplitude of the 2nd harmonic component of the sound radiated from a resonant bubble}}{\textit{amplitude of the sound exciting the bubble to resonance}}$$

Attenuation in the medium surrounding the bubbles is negligible and is ignored. Because of the nonlinearity of the system, the scattering efficiency increases with the amplitude of the driving signal (the sound transmitted by the projector) as harmonic components become more prominent in the bubble's response. Given the output of the signal synthesizer (a maximum of 10 V peak-peak) and the TVR of the chosen projector, the maximum driving signal amplitude can be more than 1 bar at frequencies near the projector's main resonance peak at 150 kHz. This presents a problem in the analysis. The model chosen for estimating the

amplitude of radiated sound from a resonant bubble is given by Prosperetti (1974)*. This is an analytic solution to the governing equations that has been obtained using perturbative expansions of their terms, and therefore is valid only for sufficiently small deviations from equilibrium. It typically gives nonsensical results when the driving amplitude is made higher than a few tenths of a bar. Our approach to applying the model is to use it to compute the scattering efficiency at a driving amplitude sufficiently low that the model is valid, then to extrapolate to higher driving amplitudes. The amplitude of the 2nd harmonic distortion component in the sound radiated from a resonant bubble is proportional (in theory) to the square of the driving amplitude.

Accordingly, the scattering efficiency is estimated for bubbles resonating at the frequencies of interest at a constant driving amplitude of 0.5 millibar (mbar), and this result is extrapolated to all other amplitudes. The bubble is assumed to be 3 cm from the hydrophone face. Because resonant bubbles are essentially monopole radiators, the pressure amplitude of the radiated sound is inversely proportional to distance. The scattering efficiency is evaluated only at the main resonance frequency for each bubble. It is dependent on raising the bubble diameter to the 1.65 power, rather than the 1.0 power that the simplest analysis would suggest; weaker damping for larger resonant bubbles probably is the explanation (Prosperetti 1977).

---

* The model was checked for accuracy by comparing its predictions of the amplitude of the bubble wall displacement to numerical solutions of more detailed (and presumably, more accurate) expressions of the governing equations, after Prosperetti et al. (1988) and Kamath and Prosperetti (1989). Agreement was satisfactory (Albin et al.,1992).

The above information on transducer gains and bubble dynamics is combined to calculate the voltage at the hydrophone, given input voltages to the projector of 1 to 10 V P-P. The results, presented in dBm (dB *re* 1 mWrms @ 50 Ω), are shown in Figures 3 and 4. The signal is predicted to weaken with decreasing frequency because of the steep roll-off of the projector response, even though larger bubbles are excited to resonance at lower frequencies. The maximum expected variation of signal strength with frequency, at a given input voltage, is 77 dB.

The results in Figures 3 and 4 are for a single bubble. Multiple-bubble dynamics are complicated, but theory indicates that a group of bubbles resonating at a given frequency should have a larger scattering cross section than a single, larger bubble resonating at the same frequency (d'Agostino and Brennan 1988). So, the displayed results are probably conservative, that is, for a group of bubbles resonating at a given frequency the output voltage would be higher than for a single bubble resonating at the same frequency.

To estimate the highest voltage likely to be encountered at the hydrophone, we can repeat the above computations with some frequency-invariant scattering efficiency that represents the maximum energy that would ever be transferred from the one transducer to the other. (Note that this time we are concerned with the combined energy of all components of the signal, not just the 2nd harmonic component). A scattering efficiency of unity means no transmission loss at all and is unrealistic; we do not know just what is the best value to use. In Figure 5 results are shown for a scattering efficiency of 0.1 (i.e., 20 dB of transmission loss). The signal levels again are expressed in dBm. It is expected that actual losses will be greater, so the estimates in Figure 5 are thought to be conservative.

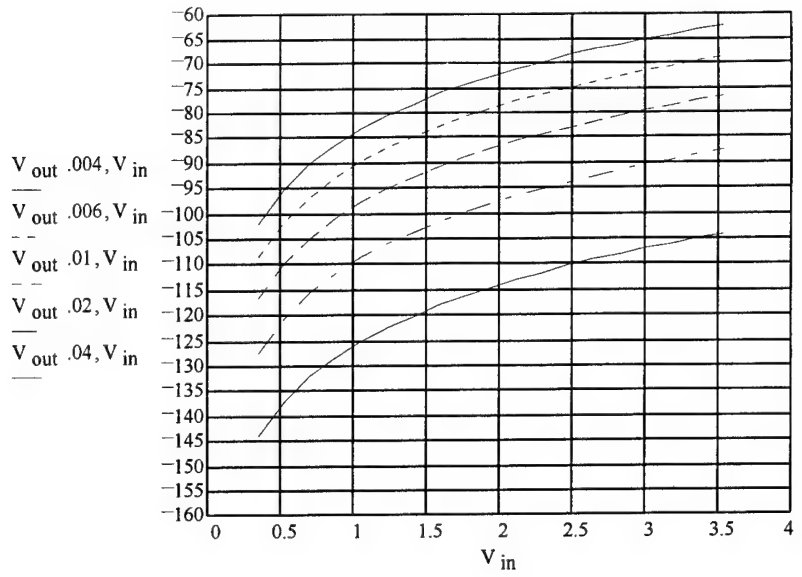

Figure 3: Expected 2nd harmonic of the output voltage in dBm as a function of input rms voltage when the target is a single bubble of diameter 40, 60, 100, 200, and 400 microns.

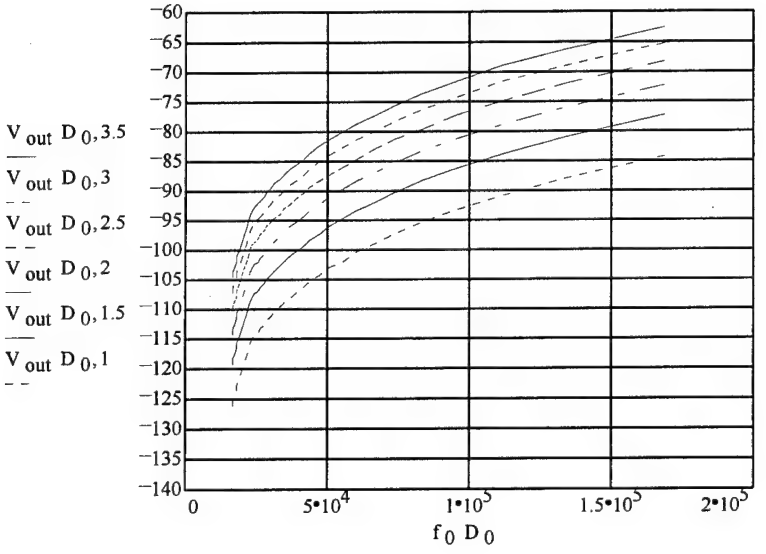

Figure 4: Expected 2nd harmonic of the output voltage as a function of frequency at input voltages of 1 to 3.5 Vrms, assuming a single bubble that resonates at the frequency of interest

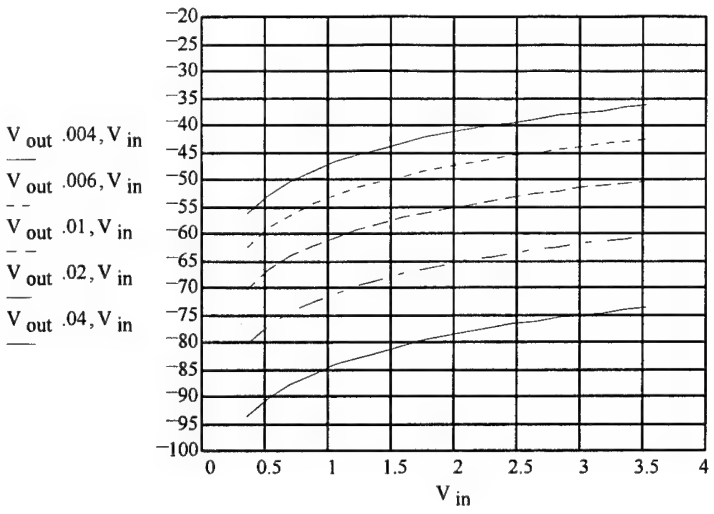

Figure 5: Excpected fundamental of the output voltage in dBm as a function of input voltage; for input signal frequencies of 16-168 kHz

The required dynamic range at a given frequency, in dB, is found simply by subtracting the minimum y-value at any frequency in Figure 3 from the maximum y-value at any frequency in Figure 5 (at the same voltage, of course): the answer ranges from about 68 dB at 10 V input to 88 dB at 1 V input.

Note that the noise floor is composed of both harmonic distortion, whose level usually is roughly proportional to the signal level, and white noise, whose level is independent of signal level. This means that a suitable set of components must have at least two characteristics: (1) they must have harmonic distortion figures substantially better than 68 dB below the fundamental, or else their internally generated distortion would mask the signals of interest, and (2) they must not saturate unless the signal level is substantially more than 68 dB above than the white noise floor.

Do the candidate components meet these constraints? To answer that question, we must sum the noise contributions from the components and calculate the attainable dynamic range of the overall system. First, we evaluate the thermal contribution to the white noise; this is the irreducible part of the noise floor. The thermal noise contribution is 3.2 nVrms per root Hz at 25°C. The "Hz" in this equation is the operating bandwidth in Hz; it will be limited to about 200 kHz by the projector's voltage response. At 25°C the thermal noise over this bandwidth is -104 dBm.

The contribution of the transducers to noise and distortion is unknown and will have to be ignored. The cumulative noise from the synthesizer, amplifier, and mixer is no more

than -84 dBm*. The system's headroom is limited by the mixer, and the lowest-power mixer overloads at +1 dBm at the RF port; the highest-power mixer overloads at +15 dBm. Therefore, the available dynamic range is limited by noise to no more than 85 to 99 dB, depending on which mixer is in line and neglecting the transducers.

The sum of the contributions made by the individual components to 2nd harmonic distortion is found to be -70 dB of *re* the fundamental, so dynamic range is limited by distortion to 70 dB. The last component in the signal path is the 3561A signal analyzer; it has a claimed dynamic range of 80 dB and therefore is not a factor in the analysis.

We have noted that the *required* dynamic range is no less than 68 dB, calculated at the maximum available input voltage. This is not comfortably smaller than the available dynamic range. However, it can easily be decreased by low-pass filtering at the hydrophone output. This works because the required dynamic range is computed correctly by subtracting the maximum noise level from the minimum level of the desired signal. Fortuitously, the minimum signal level occurs at the lowest frequency, while the maximum noise level occurs at the highest frequency, so a low-pass filter selectively reduces noise relative to signal. The magnitude of reduction in the required dynamic range is simple to compute: The assumed operating band is roughly 3.5 octaves, so a well-chosen single-pole filter (6 dB/octave rolloff) can yield up to 21 dB of improvement, a two-pole filter yields up to 42 dB improvement, etc. The chosen pre-amplifier has a suitable low-pass filter with selectable cutoff.

---

* It may be useful to illustrate how this result was calculated. There is -104 dBm of thermal noise and -90 dBm contributed by the signal source, and the amplifier contributes -102 dBm over a 200 kHz operating bandwidth. These numbers are converted to linear scale and the square root of the sum of their squares is found to be -90 dBm (after reconverting to logarithmic scale). The mixer adds 6 dB (not dBm) to that, bringing the total to -84 dBm. The overall harmonic distortion is calculated simply as the sum of the individual components' contributions (after converting their distortion figures to linear scale).

Since the required dynamic range can be made much less than the available dynamic range of at least 70 dB, we conclude that the system should be sensitive enough to detect bubbles of the sizes for which the calculations were done, barring unexpectedly large noise or distortion from the transducers.

Whereas the preceding analysis indicates that the S/N ratio would be poor at frequencies on the order of 1 MHz and higher, it is reasonable to ask why adequate sensitivity is routinely achieved at such frequencies in Doppler-based detection of intravascular bubbles. The first reason is that the Doppler signal is processed so that sound reflected from stationary reflectors does not contribute to the output. Background noise is therefore minimal, as there are no hard reflecting surfaces in the blood. The second reason is that Doppler monitoring for intravascular bubbles is done by having a human observer listen to the output signal. A human brain is used to discriminate signal from noise, and a brain is superior to any electronic signal processor at resolving the time and frequency information in sound.

Safety issues must be considered before we concluded that the input power levels assumed in the above discussion are acceptable. The potential for noise-induced hearing loss is one of those issues, and so we must estimate how loud the projector might be at the inner ear. The maximum sound pressure level (SPL) *re* 1 μPa*, measured 3 cm from the projector in water for a 10 V P-P input, is 194 dB at 50 kHz and 173 dB at 20 kHz. Suppose that sound could be transmitted from water to air without reflection at the phase boundary. Then there would be no loss of intensity between the phases, with intensity defined as the rate of energy transfer per unit area and given by

* The reference pressure amplitude commonly used when designating an SPL in water is 1 μPa rms. In air, the usual reference amplitude is 20 μPa rms.

$$I = (P_{rms})^2/\rho c$$

where P_{rms} is the rms pressure amplitude, ρ is the density, and c is the propagation velocity. In the absence of transmission loss, the water-borne sound waves would be converted to sound waves in air having an SPL of 132 dB at 50 kHz and 111 dB at 20 kHz, *re* 20 μPa. As noted before, for intracorporeal transmission the signal will be attenuated by at least 48 dB between the projector and the inner ear, and so transmission by this pathway poses no appreciable auditory hazard. The amount of sound that will be leaked into air from the projector housing is impossible to predict. It would have to be determined empirically with a sound level meter, and if found to be excessive, the subject and operator would have to wear ear protection, which is quite effective at the higher audible frequencies. It *is* possible to place *a priori* an upper bound on exposure by this path. The maximum total energy generated within the 15-20 kHz band for a 0.2-second sweep from 15 to 150 kHz is computed by time-integrating the rate of energy transfer through a closed spherical shell by a spherical wave (Kinsler et al., 1982). In this calculation, the frequency-dependent pressure amplitude is taken from the TVR data. It is found that no more than $2 \cdot 10^{-7}$ J can be generated per sweep over audible frequencies, and no more than 0.1 J over all frequencies. Whereas exposure to noise in the workplace is thought to present a hazard only when the energy density in air is some thousands of $J \cdot m^{-2}$, so air transmission will pose no appreciable risk to hearing.

Another measure of potential risk is the spatial peak pulse average (SPPA) sound intensity. The spatial peak temporal average (SPTA) is simply the SPPA multiplied by (pulse duration/pulse repetition period) and is therefore some fraction of the SPPA. The medical

community has widely accepted 100 $mW \cdot cm^{-2}$ a safe SPTA level (Miller, 1991; Duck and Martin, 1991). The SPPA intensity generated by this system cannot exceed 1 $mW \cdot cm^{-2}$.

Rectified diffusion can be ruled out as a hazard if the product of pulse length and pulse repetition frequency is small enough. It is anticipated that this product will be quite small, e.g., a 0.2-second sweep once per minute. The possibility of cavitation cannot be dismissed entirely, but it would appear to be small. The highest sonic amplitude that can be generated is 1.4 bar peak. This might lead to cavitation in tissue that is nearly saturated or supersaturated. However, for a 0.2-second sweep the length of time during which the sonic amplitude is greater than 1 bar peak is only 0.02 s. To put that in perspective, supersaturation in the tissues of human divers is thought to cause cavitation and bubble growth. The amount of supersaturation (the "overpressure") is probably on the order of 0.1 to 1 bar, but it exists for periods on the order of 1 min to 1 h.

The above analysis suggests that, if the system is to be sufficiently sensitive to a single bubble, the operating frequencies cannot be much higher than the those assumed in the calculations. The output signal level would decline by 33 dB for every tenfold increase in frequency. This loss of sensitivity could be counteracted by the insertion of a low-distortion power amplifier to boost the input to the projector by 16.5 dB per tenfold increase in frequency, but it is not unambiguously desirable to project more energy into the tissue because of the possible health hazards. For example, an increase of 16.5 dB in the input power translates into a seven-fold increase in the acoustic pressure amplitude; cavitation would be an expected side effect. Another likely effect of high sound amplitudes would be

the fracture of some bubbles into smaller bubbles; this is what probably would happen to bubbles in anisotropic media during high-amplitude, non-spherically symmetric oscillations.

A cloud of bubbles

What if a cloud of bubbles is scattering energy, rather than a single bubble? The analysis of clouds of same-sized bubbles (d'Agostino and Brennan, 1988) shows that the scattering cross section of a cloud is smaller than, but of the same order of magnitude as the sum of the cross sections of the individual bubbles that make up the cloud. The resonance frequency of the cloud is lower than that of an individual bubble, though for void fractions that might plausibly be expected in tissue, for instance <0.01%, the cloud's main resonance frequency is not too much different from that of a single bubble. The cloud's natural frequency is found to be a function of bubble size, the number density of bubbles, and the volume of the cloud.

It appears that no one has developed a theoretical description of how swept-frequency sound is scattered by a cloud of different-sized bubbles. Scattering must be maximized at the natural frequency of the cloud, but what happens at the natural frequencies of individual bubbles? Are there additional maxima in the scattering cross section at those frequencies?

Suppose the cloud behaves in the simplest conceivable manner, by scattering a significant amount of incident sound only at its own natural frequency. Then how would the cloud's scattering cross section be affected by incident sound of non-uniform amplitude throughout the cloud, as would be realized if the projector is not perfectly nondirectional? This is an important consideration if one wants to distinguish, say, a dense cloud of small

bubbles from a sparse cloud of large bubbles. They might resonate at the same frequency and would be distinguishable only because they scatter different amounts of sound.

The behavior of bubble clouds when excited to oscillation is a relatively new field of study. It is not obvious how the energy backscattered by a bubble cloud in a real world experiment should be interpreted to yield quantitative information about the size of the cloud and the size of the bubbles. Of course, it is not known whether bubble cloud dynamics would be important at all in the interrogation of bubbles *ex vivo* after dives.

FEASIBILITY OF USING TIME DELAY SPECTROMETRY AT LOW FREQUENCIES

As demonstrated in the preceding section, a sufficiently high S/N ratio apparently necessitates operating the TDS bubble detector at what we will call "low" frequencies, e.g. input frequencies of no more than a few hundred kHz. However, the requirement of adequate spatial resolution is not met at low frequencies. Spatial resolution becomes an issue when one attempts a measurement in the presence of reflecting surfaces (other than the bubble) that are too close to the bubbles. In the following section we quantify the problem and discuss the strategies we have considered for circumventing the problem.

Calculating the available spatial resolution

Let us consider the factors that determine the spatial resolution of the bubble detector. The following discussion is specific to the HP 3561A signal analyzer, but it will be shown later that the spatial resolution would be essentially the same for any other ADC/FFT (analog to digital conversion fast fourier transform) device.

The bandwidth of the captured signals is called the "span". The user normally wants the signal analyzer to capture the output signal only while the signal generator is performing a scan; in other words, the "time record" captured by the analyzer should be the same length as the scan time. The span therefore is chosen to ensure this, as will be shown now.

Like most commercially available digital signal analyzers, the 3561A collects 2^{10}=1024 digital samples per time record. The sample rate is thereby determined:

$$\text{sample rate} = (1024 \text{ samples})/(\text{length of time record}) \qquad [2]$$

The sample rate always equals 2.56·span. (In theory, it could be as low as 2.0·span, the Nyqvist frequency. The higher sample rate is a concession to the finite rolloff rate of the analyzer's analogue anti-aliasing filter.) Since it is desired that the time record length equal the sweep time, we see by inspection that

$$\text{span} = 400/(\text{scan time}) \qquad [3]$$

where the span is in Hz and the sweep time is in sec. There are 400 lines computed in the Fourier transformation, so the distance between lines equals (span ÷ 400).

A formula adapted from Reference 1 gives the bandwidth of signals received from acoustical targets within some range of distances:

$$\Delta f_{offset} = \frac{\Delta f_{scan} \cdot \Delta d}{(\text{scan time, sec}) \cdot c} \qquad [4]$$

where Δf_{scan} = bandwidth of scan, Hz;
Δd = spatial resolution, cm;
c = velocity of sound, ~$1.5 \cdot 10^5$ cm·sec^{-1} in water.

The relevant value of Δf_{offset} is the span to which the signal analyzer is set. Substituting "span" for Δf_{offset} in Equation 4 and combining Equations 3 and 4 yields

$$\Delta d = \frac{(400 \text{ Hz}\cdot\text{sec})\cdot c}{\Delta f_{scan}} \qquad [5]$$

Note that Δd is independent of the span and the scan time. This is because both the span and the distance between spectral lines are inversely proportional to the scan time.

If one substitutes a scan bandwidth of Δf_{scan} = 200 kHz, a spatial resolution of Δd = 300 cm is computed. This clearly is not suitable for interrogating biological samples.

Representative experimental results from a TDS bubble detector

An experimental bubble detector was assembled. It consisted of the components listed in the section "Selecting the hardware". In a water tank, sound from the projector was reflected off of a hard surface on its way to the hydrophone to simulate the reflections from hard surfaces that would be expected when interrogating tissue. Figure 6 shows the apparent frequency response during a sweep from 200 kHz to 10 kHz. In the absence of multipath arrivals, the response would decline sharply from left to right. The observed, more gentle decline indicates that multipath arrivals are causing sound to "accumulate" during the sweep. The lumpiness of the frequency response arises from interference between signals of different frequencies.

Figure 7 shows the range information for the same sweep. Although only one reflecting target was present, multiple peaks are evident, indicating multipath arrivals.

(It was intended that the experimental system be used to detect bubbles generated by gas injection into a liquid through small-bore [<1 μm diameter] micropipettes, with independent measurement of the bubble sizes. Attempts to do this were unsuccessful; we were not able to generate bubbles small enough that they resonated at frequencies at which the hydrophone responds.)

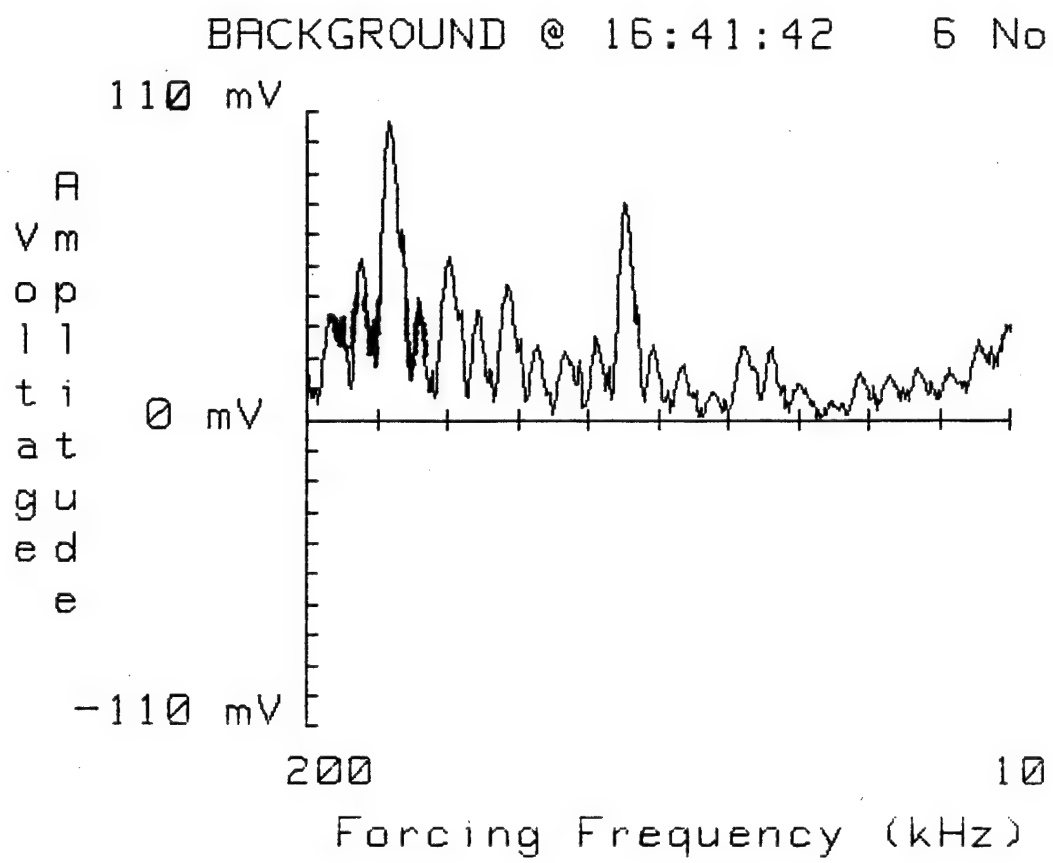

POSITIVE AREA IS 4043.37 millivolts-kHz
NEGATIVE AREA IS +0.00 millivolts-kHz

Figure 6: Apparent frequency response of the redesigned bubble detector when the projected sound is reflected toward the hydrophone from a hard target.

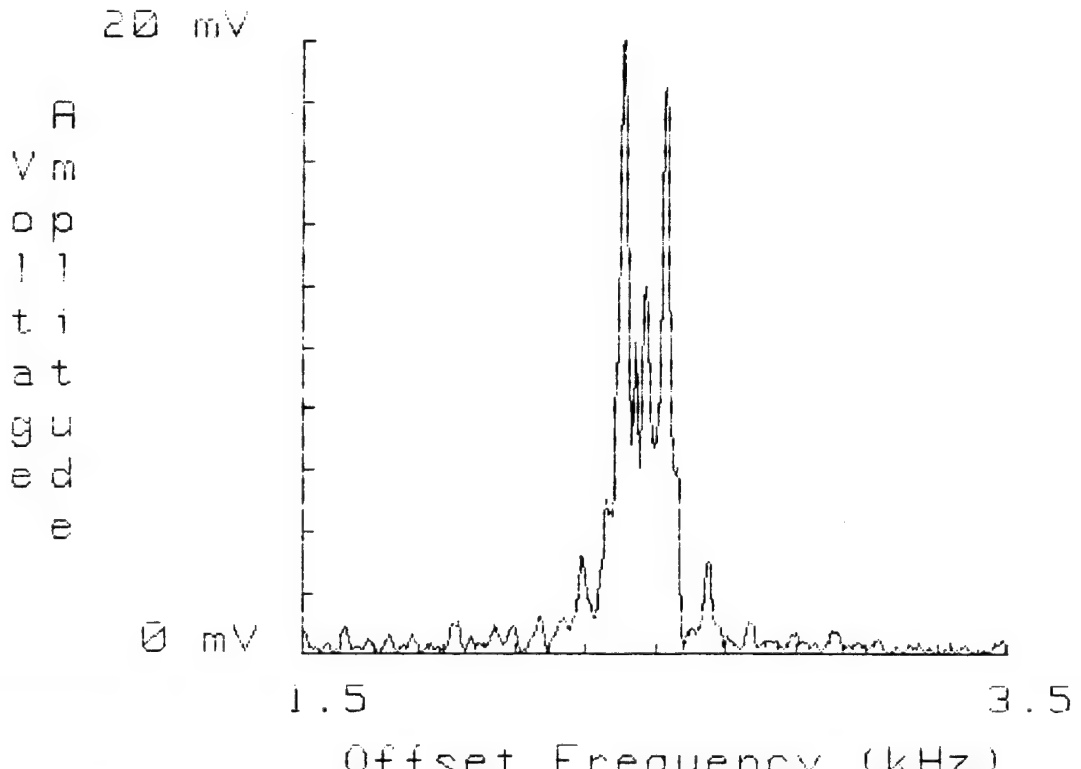

Figure 7: Output of the redesigned bubble detector operated in the "range" mode for same experiment.

Strategies for improving the spatial resolution

Some fundamentals of digital spectral analysis will be reviewed. Then, we will discuss specific strategies that have been considered for improving the spatial resolution of the TDS bubble detector.

An ADC/FFT device takes N samples over time Δt. The quantity Δt is the time resolution of the measurement; changes in the frequency content that occur over shorter times cannot be resolved. The sample rate is

$$\text{rate} = N/\Delta t \qquad [6]$$

The maximum theoretical bandwidth is

$$\text{band} = \text{rate}/2 \qquad [7]$$

The maximum number of spectral lines

$$n_{lines} = N/2 \qquad [8]$$

The distance between lines is the frequency resolution of the spectrum; it is given by

$$\Delta f = \text{band}/n_{lines} \qquad [9]$$

The combination of Equations 6-9 reveals the inverse proportionality between time and frequency resolution:

$$\Delta t \cdot \Delta f = 1 \qquad [10]$$

This is an uncertainty principle that applies to Fourier transformation as a time/frequency signal analysis tool. There are other time/frequency analysis techniques that can give better resolution in both domains.

Equation 5 shows what factors determine the spatial resolution of a TDS system. For interrogating biological samples, one might expect the necessary resolution to be no more

than 2 cm, which is about 150× better than that of the proposed bubble detector. Can the spatial resolution of that system be improved?

Obviously, the scan bandwidth can be widened. Although we expect that the chosen projector's useful response extends to only about 200 kHz, we might sweep its input voltage over a 30 MHz band. This would deliver spatial resolution of 2 cm. However, the signal analyzer has only 400 lines in the amplitude spectrum after Fourier transformation (the theoretical maximum, given 1024 samples per time record, is 512 lines). This means less than three of the lines would represent the band in which useful information might be expected. Although it is possible to digitally filter out the other 397 lines and amplitude demodulate the remaining three, it would be a pointless exercise: there is insufficient frequency resolution.

Then, we could choose transducers with wide enough operating bands that useful information would be contained across the whole 400 lines of the spectrum. A piezoelectric projector has a useful response only over some finite number of octaves (e.g., we would expect the chosen projector to be useful from about 10 to 200 kHz, or about 4.3 octaves). Because the sensitivity of a transducer is not a function of its resonance frequency, the number of useful octaves does not depend on the resonance frequency, either; so the operating bandwidth increases in proportion to the resonance frequency. Adequate spatial resolution therefore could be achieved with a projector that responds to frequencies 150× higher than the one in the proposed bubble detector. However, this would entail a loss of 72 dB in the output signal level, which could be counteracted only by a 36 dB boost in the scanning signal level. This means a 62-fold increase in the sound amplitude, which is not tolerable.

If the frequency resolution is inversely proportional to the number of samples, then would a higher sample rate be advantageous? No, because a higher sample rate increases the bandwidth of the frequencies that can be resolved, without decreasing the distance between lines in the spectrum. The frequency resolution remains the same.

How about making the time record longer than the scan time? This would reduce the span (see Equation 3) so that the indirect signals could be excluded from the passband. If the time record were lengthened by 150× without changing the scan time, the span would narrow by 150×, and the desired spatial resolution would be realized. Again, however, this would leave less than three of the 400 spectral lines representing the period during which the sample is scanned, and meaningful information could not be gotten from the demodulation.

Apparently, there is no way to gain spatial resolution in the digital domain. Suppose analogue bandpass filtering is used instead to reject indirect signals -- how narrow would the passband have to be?. The widest desired passband (meaning, the band that includes direct signals only) is obtained when the signal generator is swept through the scanning frequencies as fast as possible. With the HP 3326A, the shortest sweep time is 0.05 sec. From Equation 4, for spatial resolution Δd of 2 cm and a scanning bandwidth Δf_{scan} of 200 kHz, the desired passband is 53 Hz.

In theory, this could mean a single low-pass filter with a cutoff of about 50 Hz. In practice, because of the large near-DC noise component generated within any digital signal analyzer and the 60-Hz power line noise, it is necessary to shift up the signal frequencies by a few hundred Hz. This can be accomplished by introducing an offset between channels A and B on the signal generator (see Figure 2), so that when channel A generate a voltage at

frequency f_s, channel B is generating voltage at frequency $2 \cdot f_s + \delta f_s$, where δf_s is a few hundred Hz. The desired signals are then centered around δf_s. For instance, if δf_s is 300 Hz, then the passband should be about 275 to 325 Hz. Filtering around such a narrow band would be difficult.

A NON-TDS SYSTEM PERMITTING SUCCESSFUL LOW-FREQUENCY OPERATION, BUT WITHOUT SPATIAL RESOLUTION

Our analysis indicates that it is possible to build a system that is sensitive enough to acoustically detect bubbles by driving them to resonance, but the TDS technique appears inappropriate for that purpose. One might therefore consider building a non-TDS bubble detector. At least two possible approaches come to mind; they both dispense with the heterodyning, and therefore have the disadvantage of not providing information on the locations of bubbles.

At least one digital signal analyzer (the HP 89410) is now available that can resolve frequencies from DC to 10 MHz. This could be used for detecting the 2nd harmonic component of the sound radiated by bubbles that resonate at frequencies of up to 5 MHz (5 MHz being the main resonance frequency of a 2 μm-diameter bubble) without the use of heterodyning to downconvert the signal to a lower frequency. The mode of operation could be to sweep the input signal through a frequency band of interest with the signal analyzer tuned to twice that band. This way, the fundamental would be rejected automatically. For instance, the scanning signal might be swept from 20 to 40 kHz, to excite resonances in bubbles between about 160 and 330 μm, with the analyzer tuned to the 40 to 80 kHz band.

None of the fundamental would show up in the spectrum because there is no overlap between the scanning frequencies and the analyzer's passband. An obvious drawback is that only one octave at a time could be covered; covering the 10 to 200 kHz range would require five separate scans. Another drawback is that the 3rd harmonic would not always be rejected, although obviously this could be achieved by scanning and analyzing over more narrow bands (e.g., scanning from 20 to 30 kHz and analyzing the 40 to 60 kHz band).

A better idea might be to sweep over the entire band of interest at once, and resolve the amplitude of the scattered energy in the time/frequency plane using one of the Cohen class of time/frequency distributions (Boashash 1992), in place of Fourier transformation. These distributions are useful for analyzing signals having time-varying frequency content. In particular, the Wigner and Choi-Williams distributions work well with linear swept-frequency signals. They offer better resolution in both the time and frequency domains than is possible with Fourier transformation. It should be possible with a Cohen-class distribution to filter out the unwanted harmonics, which would appear in the time/frequency plane as straight lines having different slopes and intercepts than the 2nd harmonic.

CONCLUDING REMARKS

The analysis presented in this report indicates that TDS is not a viable choice for acoustically detecting bubbles in tissue. This statement will remain true until the sensitivity of hydrophones is improved sufficiently to overcome the poor signal/noise ratio at frequencies on the order of 10^6, where bubbles smaller than 10 μm resonate. Whether bubbles that small exist for extended periods in tissue is unknown.

REFERENCES

Albin, G., Massell, P., and Thalmann, E., Basic Operation and Preliminary Trials of a Detector for Stationary Gas Bubbles, Naval Medical Research Institute Technical Report 91-39, 1991.

Albin, G., Massell, P., Mints, W., and Himm, J. A Detector for Stationary Gas Bubbles: Feasibility Studies, NMRI Technical Report No. 92-25, Naval Medical Research Institute, Bethesda, MD, 1992.

Atchley, A.A., Frizzell, L.A., Apfel, R.E., Holland, C.K., and Madanshetty, S., and Roy, R.A., "Thresholds for cavitation produced in water by pulsed ultrasound." Ultrasonics, Vol. 26, pp. 280-285, 1988.

Atchley, A.A., "Acoustic cavitation and bubble dynamics." Chapter 1, Ultrasound: Its chemical, physical, and biological effects, edited by Suslick K.S., V.C.H. Publishers, New York, 1988.

Atchley, A.A., "The Blake threshold of a cavitation nucleus having a radius-dependent surface tension." Journal of the Acoustical Society of America, Vol. 85, pp. 152-157, 1989.

Atchley, A.A. and Prosperetti, A., "The crevice model of bubble nucleation." Journal of the Acoustical Society of America, Vol. 86, pp. 1065-1084, 1989.

Boashash, B., editor, Time frequency signal analysis: Methods and applications, Longman Cheshire, Melbourne, 1992.

Bobber R.J., Underwater electroacoustic measurements, Naval Research Laboratory, Washington, D.C., 1970.

Buddemeyer, E.U., "The physics of diagnostic ultrasound." Radiologic Clinics of North America, Vol. 13, pp. 391-402, 1975.

Crum, L.A., Roy, R.A., Dinno, M.A., Church, C.C, Apfel, R.E., Holland, C.K., and Madanshetty, S.I., "Acoustic cavitation produced by microsecond pulses of ultrasound: A discussion of some selected results." Journal of the Acoustical Society of America, Vol. 91, pp. 1113-1119, 1992.

Daft, C.M.W., Briggs, G.A.D., and O'Brien, W.D., Jr., "Frequency dependence of tissue attenuation measured by acoustic microscopy." Journal of the Acoustical Society of America, Vol. 85, pp. 2194-2201, 1989.

d'Agostino, L. and Brennan, C.E., "Acoustical absorption and scattering cross sections of spherical bubble clouds." Journal of the Acoustical Society of America, Vol. 84, pp. 2126-2134, 1988.

d'Agostino, L. and Brennan, C.E., "Linearized dynamics of spherical bubble clouds." Journal of Fluid Mechanics, Vol. 199, pp. 155-176, 1989.

Dallos, P., "Nonlinear distortion." Chapter 6, The Auditory Periphery; Biophysics and Physiology, Academic Press, New York, 1973.

Duck, F.A. and Martin, K., "Trends in ultrasound exposure." Physics in Medicine and Biology, Vol. 36, pp. 1423-1432, 1991.

Francis, T.J.R., Pezeshkpour, G.H., Dutka, A.J., Hallenbeck, J.M., and Flynn, E.T., "Is there a role for the autochthonous bubble in the pathogenesis of spinal cord decompression sickness?" Journal of Neuropathology and Experimental Neurology, Vol. 47, pp. 475-487, 1988.

Francis, T.J.R., Griffin, L., Homer, L.D., Pezeshkpour, G.H., Dutka, A.J., and Flynn, E.T., "Bubble-induced dysfunction in acute spinal cord decompression sickness." Journal of Applied Physiology, Vol. 68, pp. 1368-1375, 1990.

Gersh, I., "Gas bubbles in bone and associated structures, lung and spleen of guinea pigs decompressed rapidly from high pressure atmospheres." Journal of Cellular and Comparative Physiology, Vol. 26, pp. 101-117, 1945.

Goss, S.A., Johnston, R.L., and Dunn ,F., "Compilation of empirical ultrasonic properties of mammalian tissues. II." Journal of the Acoustical Society of America, Vol. 68, pp. 93-108, 1980.

Hills, B.A. and Butler, B.D., "Size distribution of intravascular air emboli produced by decompression." Undersea Biomedical Research, Vol. 8, pp. 163-170, 1981.

Kamath, V. and Prosperetti, A., "Numerical integration methods in gas-bubble dynamics." Journal of the Acoustical Society of America, Vol. 85, pp. 1538-1548, 1989.

Kinsler, L.E., Frey, A.R., Coppens, A.B., and Sanders J.V., Fundamentals of acoustics, John Wiley and Sons, New York, 1982.

Kumar, S. and Brennan, C.E., "Nonlinear effects in the dynamics of clouds of bubbles." Journal of the Acoustical Society of America, Vol. 89, pp. 707-714, 1991.

Lu N.Q., Prosperetti A., and Yoon S.K., "Underwater noise emissions from bubble clouds." IEEE Journal of Oceanic Engineering, Vol. 15, pp. 275-281, 1990.

Miller, D.L., "Update on safety of diagnostic ultrasonography." Journal of Clinical Ultrasound, Vol. 19, pp. 531-540, 1991.

Omta, R., "Oscillations of a cloud of bubbles of small and not so small amplitude." Journal of the Acoustical Society of America, Vol. 82, pp. 1018-1033, 1987.

Price, G.R. and Kalb, J.T., "Insights into hazard from intense impulses from a mathematical model of the ear." Journal of the Acoustical Society of America, Vol. 90, pp. 219-227, 1991.

Price, G.R., "Importance of spectrum for rating hazard: Theoretical basis," Chapter 31, Noise-Induced Hearing Loss, edited by Dancer A.L., Mosby-Year Book, St. Louis, MO, 1992.

Prosperetti, A., "Thermal effects and damping mechanisms in the forced radial oscillations of gas bubbles in liquids." Journal of the Acoustical Society of America, Vol. 61, pp. 17-27, 1977.

Prosperetti, A., "Nonlinear oscillations of gas bubbles in liquids: Steady-State Solutions." Journal of the Acoustical Society of America, Vol. 56, pp. 878-885, 1974.

Prosperetti, A., Crum, L., and Commander, K., "Nonlinear bubble dynamics." Journal of the Acoustical Society of America, Vol. 83, pp. 502-514, 1988.

Prosperetti, A., Crum, L.A., and Pumphrey, H.C., "The underwater noise of rain." Journal of Geophysical Research, Vol. 94, pp. 3255-3259, 1989.

Prosperetti, A., Lu, N.Q., and Kim, H.S., "Active and passive acoustic behavior of bubble clouds at the ocean's surface." Journal of the Acoustical Society of America, Vol. 93, pp. 3117-3127, 1993.

Sarkar, K. and Prosperetti, A., "Backscattering of underwater noise by bubble clouds." Journal of the Acoustical Society of America, Vol. 93, pp. 3128-3138, 1993.

Smereka, P. and Banerjee, S., "The dynamics of periodically driven bubble clouds." Physics of Fluids, Vol. 31, pp. 3519-3541, 1988.

Wagner, C.E., "Observations of gas bubbles in pial vessels of cats following rapid decompression from high pressure atmospheres." Journal of Neurophysiology, Vol. 8, pp. 29-32, 1945.

Yoon, S.W., Crum, L.A., Prosperetti, A., and Lu, N.Q., "An investigation of the collective oscillations of a bubble cloud." Journal of the Acoustical Society of America, Vol. 89, pp. 700-706, 1991.

APPENDIX: A Mathcad Version 3.1 Document for Calculating the Expected Output Voltage at the Hydrophone of the JPL Bubble Detector.

Assumes that the NRL F41 is the projector and the NRL E27 is the hydrophone.

First, find the natural frequency of gas bubbles in water, from linearized theory and assuming adiabiatic oscillations. Taken from Prosperetti (1974).

$\gamma := 1.4$ polytropic exponent

$P_0 := 1013250$ ambient pressure, dyn per sq cm

$\sigma := 72.75$ surface tension of air/water, dyn per cm

$\rho := 1$ density of water, g per cu cm

$D_0 := .005,.005 .. .04$ equilibrium diameter varies from 40 to 400 μm (0.004 to0.04)

$$R_0 D_0 := \frac{D_0}{2}$$

$$f_0 D_0 := \frac{\sqrt{3 \cdot \gamma \cdot P_0 \cdot 1 + 2 \cdot \frac{\sigma}{P_0 \cdot R_0 D_0} - 2 \cdot \frac{\sigma}{R_0 D_0}}}{\sqrt{\rho \cdot R_0 D_0}}$$

natural angular frequency, in rad per sec

converting to Hz

$$f_0 D_0 := \frac{f_0 D_0}{2 \cdot \pi}$$

Transducer gains in dB.

The transmitting voltage response (TVR) is for the model F41 projector and is referenced to 1 microPa per V;
the free field voltage sensitivity (FFVS) is for the model E27 hydrophone and is referenced to 1 V per microPa.

The gains are taken from typical frequency response plots supplied by NRL and are read at each of the main resonance frequencies under consideration.

The following is found to fit the TVR data well (r = 0.997):

$$TVR\ D_0 := 23.506 \cdot 1n\ f_0 D_0 - 121.39$$

The hydrophone gain is measured at twice the frequency at which the TVR is measured. It is taken to be constant, although there is actually some roll-off at the lower frequencies:

FFVS := -225

FFVS := FFVS + 10 — Arbitrarily throw in another 10 db for the hydrophone because its cable will be shorter than when the frequency response was measured (cable was 30 m long for measurement).

The actual gain realized by shortening the cable might be greater.

Converting gains to linear scale.

$$TVR\ D_0 := 10^{\frac{TRV\ D_0}{20}}$$

The TVR's are in microPascals per V;
the FFVS is in V per microPascal.

$$FFVS := 10^{\frac{FFVS}{20}}$$

The TVR's are measured in the free field at 1 m distance. The amplititude falls off with distance to the first power in the free field and is independent of distance in the near field. For a 3 cm-distant target, the frequency at which the transition between the two regimes occurs is calculable (from RJ Bobber, "Underwater Electroacoustic Measurements"):

velocity of sound

$$c := 1.5 \cdot 10^5$$

radius of transducer face

$$a := 2.5$$

target range under consideration

$$range := 3$$

frequency at which 3 cm is at the transition from near field to far field.

$$f_{trans} := \frac{range \cdot c}{\pi \cdot a^2}$$

near field contribution

$$TVR\ D_0 := TVR\ D_0 \cdot \frac{100 \cdot c}{\pi \cdot a^2 f_0 D_0} \cdot \Phi\ f_0\ D_0 - f_{tran}$$

far field contribution

$$+\ TVR\ D_0 \cdot \frac{100}{range} \cdot \Phi\ f_{trans}\ f_0\ D_0$$

The "scattering efficiency" (SE) of a bubble increases with driving signal amplitude because the system is nonlinear. A very conservative approach is to evaluate the SE at a single low value of the driving amplitude and to assume that value for computations at all higher amplitudes.

The dependence of scattering efficiency on the resonance frequency is estimated at for a driving amplitude of 0.0005 bar peak using the model by Prosperetti (1974). This number will later be corrected for the actual driving amplitudes. The following equation is found to fit the data well (r = 0.999):

$$SE\ D_0 := \exp\ 1.6381 \cdot 1n\ D_0\ -\ 0.23251$$

with the bubble diameter in cm.

Let the input signal level vary from 1 to 10 V P-P; express it as rms voltage:

$$V_i := \frac{1}{2\cdot\sqrt{2}}, \frac{1.5}{2\cdot\sqrt{2}} .. \frac{10}{2\cdot\sqrt{2}}$$

Combining all of the above information:

$P_{in}(D_0, V_{in}) := TVR(D_0) \cdot V_{in}$ input pressure amplitude, microPascals

$P_{out}(D_0, V_{in}) := SE(D_0) \cdot \frac{P_{in}(D_0, V_{in})^2}{\frac{0.0005}{\sqrt{2}} \cdot 1.01325 \cdot 10^{11}}$ output pressure amplitude, 2nd harmonic; conversion factors are involved

$V_{out}(D_0, V_{in}) := FFVS \cdot P_{out}(D_0, V_{in})$ output voltage, microvolts

$V_{ref} := \sqrt{50 \cdot 0.001}$ reference output voltage, in Vrms (re 1 mW)

$V_{out}(D_0, V_{in}) := 20 \cdot \log\left(\frac{V_{out}(D_0, V_{in})}{V_{ref}}\right)$ express the voltage in dBm, (dB re 1 mW at 50 ohms)

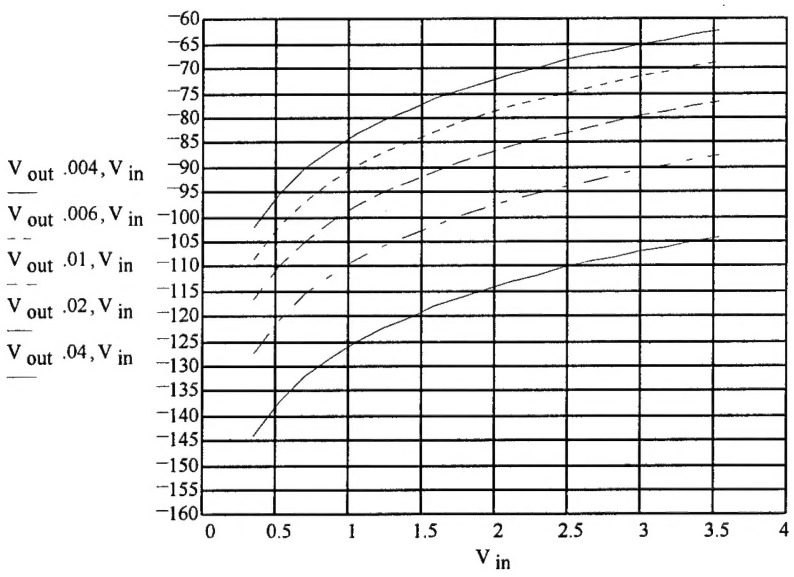

2nd harmonic of the output voltage in dBm as a function of input rms voltage when the target is a single bubble of diameter 40, 60, 100, 200, and 400 microns.

Expected output signal strength is actually higher for the smaller bubbles (higher frequencies), because of the steep rise of the F41 projector's output as the frequency increases.

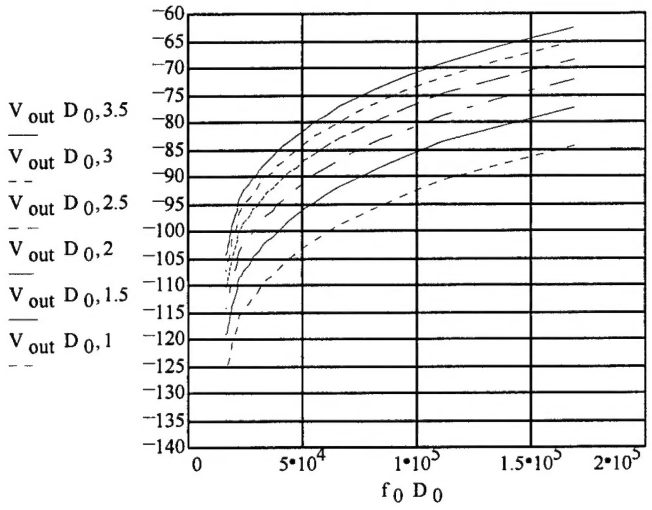

2nd harmonic of the output voltage as a function of frequency at input voltages of 1 to 3.5 Vrms, assuming a single bubble that resonates at the frequency of interest

The above computations are for a single bubble. Multiple-bubble dynamics are complicated, but theory indicates that a group of bubbles resonating at a given frequency should have a larger scattering cross section than a single, larger bubble resonating at the same frequency (d'Agostino and Brennan, 1988). So, the above results are probably conservative, that is, for a group of bubbles resonating at a given frequency, the output voltage would be stronger than for a single bubble resonating at the same frequency.

To compute the strongest conceiveable voltage at the hydrophone,
the scattering efficiency must be set equal some reasonable constant at all frequencies.
We expect that its value should be no more than 0.1:

$i := 1..17$ $\quad SE_{D_0} := 0.1$

$P_{out}(D_0, V_{in}) := SE_{D_0} \cdot P_{in}(D_0, V_{in})$

$V_{out}(D_0, V_{in}) := FFVS \cdot P_{out}(D_0, V_{in})$

$V_{out}(D_0, V_{in}) := 20 \cdot \log\left(\frac{V_{out}(D_0, V_{in})}{V_{ref}}\right)$ express the max voltage in dBm

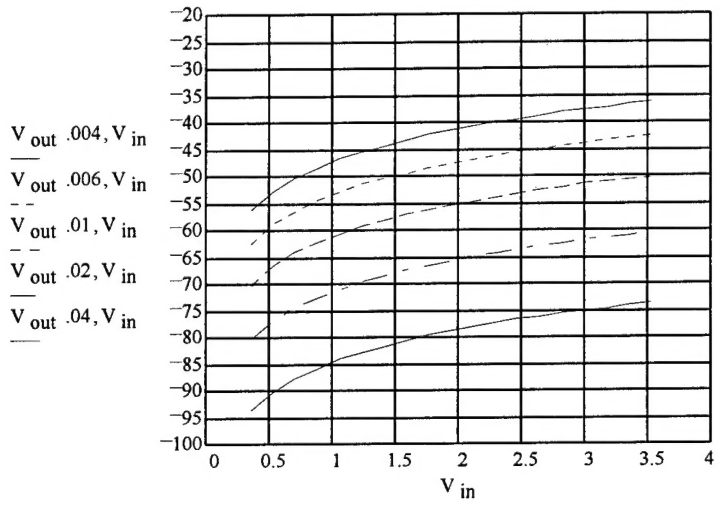

Fundamental of the output voltage in dBm as a function
of input voltage; for input signal frequencies of 16-168 kHz

About 68 to 88 dB of dynamic range is required, depending on the input voltage.

If the above exercise is repeated with a simulated 6 dB/octave low-pass filter in the signal path after the hydrophone, the required dynamic range is found to be only 47 to 67 dB, depending on the input voltage.